

# Metal Borohydrides as high- $T_c$ ambient pressure superconductors

Simone Di Cataldo<sup>1,2,†</sup> and Lilia Boeri<sup>1,3,\*</sup>

<sup>1</sup>*Dipartimento di Fisica, Sapienza Università di Roma, 00185 Roma, Italy*

<sup>2</sup>*Institute of Theoretical and Computational Physics,*

*Graz University of Technology, NAWI Graz, 8010 Graz, Austria*

<sup>3</sup>*Centro Ricerche Enrico Fermi, Via Panisperna 89 A, 00184 Rome, Italy*

(Dated: July 13, 2022)

The extreme pressures required to stabilize the recently discovered *superhydrides* represent a major obstacle to their practical application. In this paper, we propose a novel route to attain high-temperature superconductivity in hydrides at ambient pressure, by doping commercial metal borohydrides. Using first-principles calculations based on Density Functional Theory and Migdal-Éliashberg theory, we demonstrate that in  $\text{Ca}(\text{BH}_4)_2$  a moderate hole doping of 0.03 holes per formula unit, obtained through a partial replacement of Ca with monovalent K, is sufficient to achieve  $T_c$ 's as high as 110 K. The high- $T_c$  arises because of the strong electron-phonon coupling between the B-H  $\sigma$  molecular orbitals and bond-stretching phonons. Using a random sampling of large supercells to estimate the local effects of doping, we show that the required doping can be achieved without significant disruption of the electronic structure and at moderate energetic cost. Given the wide commercial availability of metal borohydrides, the ideas presented here can find prompt experimental confirmation. If successful, the synthesis of high- $T_c$  doped borohydrides will represent a formidable advancement towards technological exploitation of conventional superconductors.

## INTRODUCTION

Since the discovery of superconductivity with a critical temperature ( $T_c$ ) of 203 K at 150 GPa in  $\text{H}_3\text{S}$  [1, 2], hydrogen-rich superconductors have revolutionized the landscape of superconductivity research; After  $\text{H}_3\text{S}$ , many other superhydrides with  $T_c$ 's close to, or even above, room temperature have been found [3–12], but the extreme synthesis pressures represent an insurmountable obstacle to any practical application.

On the other hand, an increasing demand exists for new materials enabling superconductor-based technologies: for most large-scale applications, synthesizability at ambient pressure is a strict requirement, whereas the threshold for  $T_c$  is sensibly lower than ambient temperature, but is dictated by the need to maintain a robust superconducting state under liquid nitrogen cooling. [13]

The spectacular success of computational methods for superhydrides raises the hope that these techniques may accelerate the identification of suitable materials.[14, 15] The first predictions which have started to appear in literature follow essentially two different routes to boost  $T_c$  within the conventional (*ep*) scenario: 1) optimization of the effective chemical pressure in ternary hydrides [16–20], through a careful combination of guest elements in host-guest metallic superhydrides; and 2) doping of non-hydride covalent structures [21–27], which exploits the large intrinsic *ep* coupling of covalent insulators, turned metallic via either external or self doping, as in B-doped diamond or  $\text{MgB}_2$  [21, 28–30].

Both approaches present potential drawbacks: while even the most optimized ternary hydrides seem to require synthesis pressure of at least a few GPa [17], the  $T_c$ 's of systems containing exclusively boron, carbon and

other heavier elements are unlikely to exceed the 80 K threshold found in best-case scenarios [26, 27], due to the intrinsic phonon energy scales determined by the relatively large boron and carbon atomic masses.

In this paper we propose a hybrid strategy which combines the best of the two: doping covalent bonds (ambient pressure) in a hydrogen-rich structure (higher  $T_c$ ). In particular, we show that metal borohydrides (MBH) can be turned into high-temperature conventional superconductors at ambient pressure, via small substitutional doping at the metal site, which effectively transforms MBH into highly-tunable hole-doped hydrocarbons.

MBH form a broad class of materials widely used in commercial hydrogen storage applications, due to the high hydrogen content, and the ease of hydrogen uptake and dehydrogenation [31, 32]. In these compounds boron and hydrogen form quasi-molecular units arranged on open structures, with mono-, di- or trivalent metals ( $M$ ) on the interstitial sites. Our strategy to turn MBH into high- $T_c$  superconductors is quite general, and consists in replacing a small fraction of  $M$  atoms with a lower-valence atom, realising hole doping; in this work, we study the specific case of K- doping of the  $\alpha$  phase of  $\text{Ca}(\text{BH}_4)_2$  [33].

Our calculations demonstrate that substitutional K doping in  $\text{Ca}(\text{BH}_4)_2$  is energetically feasible up to at least 0.10  $\text{h}^+/\text{f.u.}$ ; concentrations as low as 0.03 holes per formula unit ( $\text{h}^+/\text{fu}$ ) are sufficient to induce superconductivity with a  $T_c$  as high as 110 K. As MBH are commercially available materials, we expect our work to find an immediate response from experimental researchers.

$\alpha\text{-Ca}(\text{BH}_4)_2$  (Fig. 1) is a molecular crystal, in which boron and hydrogen form  $\text{BH}_4$  tetrahedra, and Ca occupies interstitial sites. Ca is almost completely ionized ( $\text{Ca}^{++}$ ), and donates charge to the  $\text{BH}_4^-$  tetrahedra,

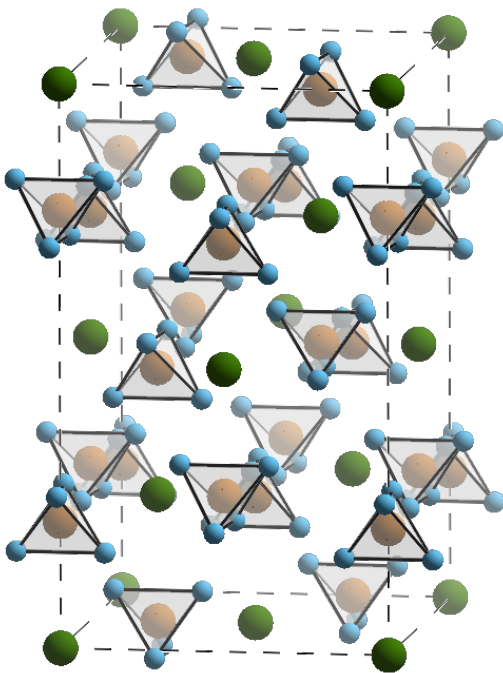


FIG. 1. Crystal structure of  $\alpha$ -Ca(BH<sub>4</sub>)<sub>2</sub>. The Ca, B, and H atoms are shown as green, orange, and blue spheres, respectively. BH<sub>4</sub><sup>-</sup> anions are shown as tetrahedra.

which are thus not only isostructural, but also isoelectronic to methane (CH<sub>4</sub>). The spacing between BH<sub>4</sub><sup>-</sup> molecular units is quite large, about 3.5 Å, indicating extremely weak intermolecular interactions.

Fig. 2 shows the electronic band structure and the atom-projected Density of States (DOS) of the  $\alpha$  phase of Ca(BH<sub>4</sub>)<sub>2</sub>. Undoped  $\alpha$ -Ca(BH<sub>4</sub>)<sub>2</sub> is an insulator, with a calculated direct band gap of 5 eV. The bands have a reduced dispersion, as typical of molecular crystals; the electronic DOS exhibits extremely sharp and narrow peaks, particularly near the valence band maximum (VBM). Electronic states in this region have a mixed (50/50) B/H character and derive from the three-fold degenerate  $1t_2$  (0 to -2 eV) and the single  $2a_1$  (-6 to -8 eV) molecular  $\sigma$  orbitals of BH<sub>4</sub>, which are expected to couple strongly to B-H bond-stretching and bond-bending, phonons.

Due to the extremely sharp profile of the DOS, even extremely small hole dopings are sufficient to shift the Fermi energy into the large-DOS, large- $ep$  region below the VBM, which should induce high- $T_c$  conventional SC.

Hole doping in Ca(BH<sub>4</sub>)<sub>2</sub> can be realized by substituting Ca with a monovalent atom. In this work, we consider K, which is the neighbour of Ca in the periodic table, and hence has very similar size and core. Replacing a fraction  $\delta$  of divalent Ca with monovalent K amounts to doping  $\alpha$ -Ca(BH<sub>4</sub>)<sub>2</sub> with  $\delta$  holes/f.u.; in an ideal rigid-band pic-

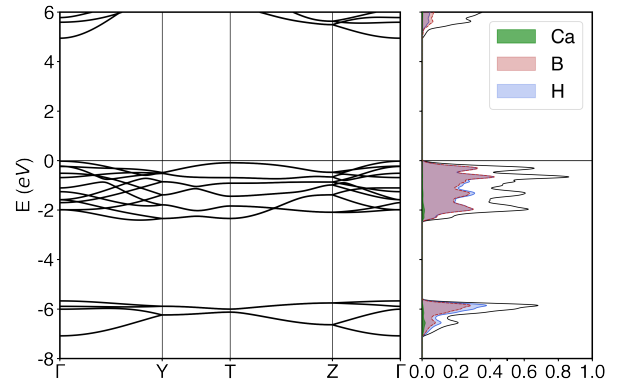


FIG. 2. Electronic band structure and atom-projected DOS of Ca(BH<sub>4</sub>)<sub>2</sub>. The energy zero is set to the valence band maximum. The DOS is in units of states  $\text{eV}^{-1}\text{atom}^{-1}$ .

ture, these holes would form at the top of the valence band, turning K-doped Ca(BH<sub>4</sub>)<sub>2</sub> into a self-doped version of methane (CH<sub>4</sub>).

Due to the presence of stiff covalent bonds coupled by symmetry to bond-stretching phonons, doped hydrocarbons have long been postulated to exhibit large  $ep$  coupling; controversial reports of high- $T_c$  superconductivity in polyacenes doped with alkali and alkaline earths (*electron* doping) have appeared in the early 2010's [34–37]. However, doping hydrocarbons and related C-H systems with *holes* has so far proven impossible, as intercalation with electronegative elements (I, F, Cl) is ineffective, and doping the C-H sublattice by substitutional atoms or vacancies is extremely unfavorable energetically and tends to seriously disrupt the crystal and electronic structure due to the presence of stiff covalent bonds [38, 39].

In K-doped Ca(BH<sub>4</sub>)<sub>2</sub>, on the other hand, doping only involves the metal site, which is very weakly bonded to the rest of the structure. This should allow a convenient fine-tuning of the superconducting properties at a reasonable energy cost, without major modifications of the structure [40].

To substantiate our hypotheses, we computed the superconducting properties of K-doped Ca(BH<sub>4</sub>)<sub>2</sub> for various hole concentrations  $\delta$ , computing the isotropic Éliashberg functions for various values of  $\delta$  using Density Functional Perturbation Theory [41], and obtaining the  $T_c$  by numerically solving the isotropic Éliashberg equations [42].

Doping is simulated using the virtual crystal approximation (VCA), which amounts to replacing each Ca (pseudo)atom in the  $\alpha$ -Ca(BH<sub>4</sub>)<sub>2</sub> structure with an average virtual (pseudo)atom, obtained by mixing K and Ca in the appropriate proportions.

In Fig. 3 we report a summary of the electronic and superconducting properties of K-doped Ca(BH<sub>4</sub>)<sub>2</sub> as a

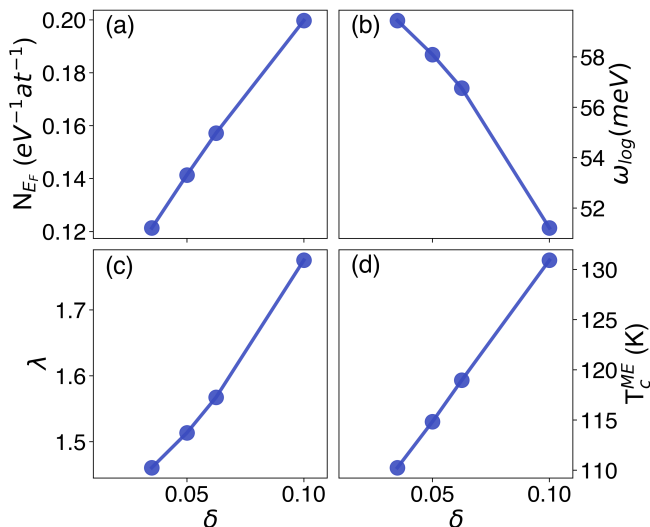


FIG. 3. Electronic and superconducting properties as a function of the doping  $\delta$ . (a): DOS at the Fermi level, (b): logarithmic average phonon frequency  $\omega_{log}$ , (c):  $ep$  coupling coefficient  $\lambda$ , (d): superconducting critical temperature  $T_c$ .

function of the hole concentration  $\delta$ . The DOS at the Fermi level  $N_{E_F}$  (panel (a)) rapidly increases with doping, as does the total  $ep$  coupling constant  $\lambda$  (panel (c)), while the average phonon frequency  $\omega_{log}$  (b) slightly decreases. In the Éliashberg function (shown in Fig. S2 of the Supplementary Material) almost all  $ep$  coupling is concentrated in the high-energy B-H stretching and bending modes. For  $\delta$  larger than 0.10 the system develops a dynamical instability, while for values smaller than 0.03 the Fermi energy is too close to the VBM to allow a reasonable estimate of  $\lambda$  and  $T_c$ .  $T_c$  attains its maximum value of 130 K at  $\delta = 0.10$  and decreases linearly with decreasing  $\delta$  down to 110 K at  $\delta = 0.03$ ; extrapolating this trend, we can reasonably suppose that  $T_c$ 's higher than 100 K may be achieved for dopings  $\delta \gtrsim 0.01$ .

The VCA has the advantage of making  $T_c$  calculations feasible even for small dopings, correctly capturing the average effect of substitutional doping on the electronic structure, in particular the critical role of electronic screening on phonon spectra and  $ep$  matrix elements. [37] However, effects such as charge localization, deep defect levels or carrier trapping [24, 43], which may sensibly affect the electronic structure, require more complex approximations that can capture depend on the local environment of the impurities.

To simulate these effects, we developed an ad-hoc scheme, based on averaging over random supercells. First, we constructed a  $2 \times 2 \times 2$  supercell containing 32 formula units of  $\text{Ca}(\text{BH}_4)_2$  (352 atoms); then, to simulate hole concentrations from  $\delta = 0.03$  to  $\delta = 0.5$ , we substituted Ca atoms with the appropriate fraction of K, placed at random positions; for each value of  $\delta$ , we gen-

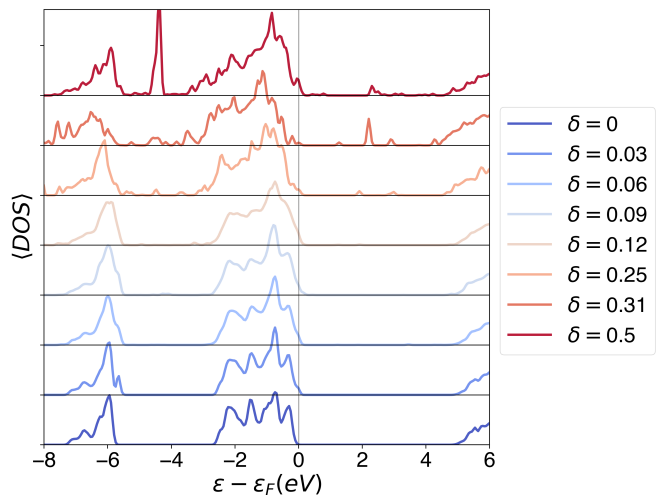


FIG. 4. Density of states (DOS) of K-doped  $\text{Ca}(\text{BH}_4)_2$  as a function of the hole concentration  $\delta$ . The Fermi energy is taken as the energy zero except for  $\delta = 0$ , in which the VBM is used.

erated ten supercells. These supercells were then relaxed to minimize stress and forces, before computing the total energies and DOS's – Figs. 4. Computations on the supercells were performed using the Vienna Ab-initio Simulation Package (VASP). Further details are provided in the Supplementary Materials [44]. The average DOS for each doping was then obtained by performing a weighted average over the relative supercells, with weights corresponding to the probability of that configuration (See SM for further details [44]). The average DOS's for different values of  $\delta$  are shown in Fig. 4. Although doping causes sizable modifications of the DOS for  $\delta > 0.12$ , especially in the low-lying region below -6 eV, the DOS for  $\delta$  up to 0.09 are essentially unchanged compared to the undoped compound. In particular, there are no inter-gap states up to  $\delta = 0.09$ , and the relative weight remains negligible up to  $\delta = 0.25$ .

Hence, for doping of interest the main effect of K/Ca substitution is indeed a quasi-rigid shift of the Fermi level into the valence band, well reproduced by VCA; in particular, the states just below the VBM, which participate in the SC pairing, are only weakly influenced by doping. This is expected, since  $\sigma$  orbitals of the  $\text{BH}_4^-$  molecular ions are only weakly affected by distortions and rearrangements of atoms in the crystal structure which do not modify the overall shape of the molecular ion itself.

Using supercells we can also estimate the energetic cost of K substitution into the Ca site. In Fig. 5 we show the formation energy of  $\text{K}_\delta\text{Ca}_{1-\delta}(\text{BH}_4)_2$  with respect to decomposition into  $\text{K} + \text{Ca}(\text{BH}_4)_2$  [45], for all configurations sampled (ten for each doping). The formation energies  $\delta E$  increase linearly with doping, with little dispersion for different supercells, remaining below 200 meV/atom for  $\delta$  up to 0.12.

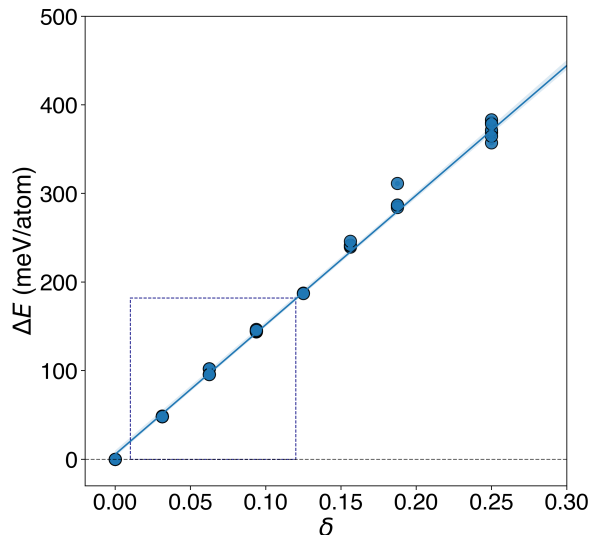


FIG. 5. Formation energy  $\Delta E$  as a function of hole-doping  $\delta$ .

On purely energetic grounds, these values indicate that K-doping of  $\text{Ca}(\text{BH}_4)_2$  should be experimentally feasible. However, experimental synthesis conditions depend on complex details of the kinetic barrier protecting the doped structure from decomposition, and on the entropy contribution to the free energy, whose evaluation goes well beyond the scope of this paper.

Moreover, independently of their energetic cost, not all perturbations induced by doping will have the same effect on superconductivity; while small distortions and rearrangements of  $\text{BH}_4^-$  anions within the open  $\alpha$  structure, should have only minor effects on the superconducting properties, dehydrogenation, which implies a weakening of the B-H bonds, has severe consequences, since it implies a major rearrangement of the whole electronic structure. We will therefore assume that the dehydrogenation energy can be used to estimate an effective synthesizability threshold for K-doped  $\text{Ca}(\text{BH}_4)_2$ .

A hand-waving estimate can be obtained as follows. Assuming the measured dehydrogenation temperature of  $\text{Ca}(\text{BH}_4)_2$ , which is around 700 K [46–48], to be a reasonable guess of the kinetic barrier for dehydrogenation, doped  $\text{Ca}(\text{BH}_4)_2$  should be able to withstand perturbations with a positive  $\Delta E$  of the order of 60 meV/atom without decomposing. This corresponds to a doping  $\delta \sim 0.06$  (Fig. 5), which as Fig. 3 (d) shows, largely exceeds the doping levels required for high- $T_c$  superconductivity. Hence, high- $T_c$  superconductivity should be observable, before dehydrogenation sets in.

In summary, in this paper we proposed a strategy to attain high- $T_c$  conventional superconductivity in the complex borohydride  $\text{Ca}(\text{BH}_4)_2$  using substitutional doping of monovalent K on the Ca site, and substantiated it with first-principles calculations.

K-doped  $\text{Ca}(\text{BH}_4)_2$  behaves essentially as hole-doped methane ( $\text{CH}_4$ ), where the high- $T_c$  derives from a strong coupling between  $\sigma$  bonding electronic states and bond-stretching phonons of the  $\text{BH}_4^-$  molecular units. Compared to  $\text{CH}_4$ , however, the big advantage of  $\text{Ca}(\text{BH}_4)_2$  is that hole doping is realized by acting on the weakly-bonded metal site, and not on the covalent B-H (or C-H) sublattice, and this causes only minor disruptions of the crystal and electronic structure, implying an affordable energy cost. According to our calculations, a partial replacement of 3 % Ca atoms with K atoms would have an energy cost of around 50 meV/atom, which is below the dehydrogenation threshold, and lead to an estimated  $T_c$  of 110 K at ambient pressure, almost on par with the best copper-oxide superconductors. With a figure of merit  $S$  between 2.8 and 3.3 [13], doped  $\text{Ca}(\text{BH}_4)_2$  is better than any other superhydride, as well as all other known ambient-pressure conventional superconductors ( $S = 1$  in  $\text{MgB}_2$ ), and very close to  $\text{HgBaCaCuO}$ .

Note that the strategy proposed here is very general, and can in principle be applied to turn any of the many existing MBH into doped hydrocarbons, by suitable metal substitutions. We are strongly convinced that, if synthesized, doped metal borohydrides will represent a huge leap forward in research on high-temperature superconductors.

Given the easy commercial availability of metal borohydrides, we hope that our work will stimulate a positive response from experimentalists.

## ACKNOWLEDGMENTS

The authors warmly thank Antonio Sanna for sharing the code to solve the isotropic Éliashberg equations. L.B. and S.d.C. acknowledge funding from the Austrian Science Fund (FWF) P30269-N36 and support from Fondo Ateneo-Sapienza 2017-2020. S.D.C. acknowledges computational resources from CINECA, proj. IsC90-HTS-TECH and IsC99-ACME-C, and the Vienna Scientific Cluster, proj. 71754 "TEST".

<sup>†</sup> simone.dicataldo@uniroma1.it

<sup>\*</sup> lilia.boeri@uniroma1.it

- [1] A. P. Drozdov, M. I. Erements, I. A. Troyan, V. Ksenofontov, and S. I. Shylin, Conventional superconductivity at 203 Kelvin at high pressures in the sulfur hydride system, *Nature* **525**, 73 (2015).
- [2] M. Einaga, M. Sakata, T. Ishikawa, K. Shimizu, M. Erements, A. P. Drozdov, I. A. Troyan, N. Hirao, and Y. Ohishi, Crystal structure of the superconducting phase of sulfur hydride, *Nature Physics* **12**, 835 (2016).
- [3] H. Liu, I. I. Haumov, Z. M. Geballe, M. Somayazulu, J. S. Tse, and R. J. Hemley, Dynamics and superconductivity

- in compressed lanthanum superhydride, *Phys. Rev. B* **98**, 100102 (2018).
- [4] M. Somayazulu, M. Ahart, A. K. Mishra, Z. M. Geballe, M. Baldini, Y. Meng, V. V. Struzhkin, and R. J. Hemley, Evidence for superconductivity above 260 K in lanthanum superhydride at Megabar pressures, *Phys. Rev. Lett.* **122**, 027001 (2019).
  - [5] A. P. Drodzov, P. P. Kong, S. P. Besedin, M. A. Kuzonikov, S. Mozaffari, L. Balicas, F. F. Balakirev, D. E. Graf, V. B. Prakapenka, E. Greenberg, D. A. Knyazev, M. Tkacz, and M. I. Eremets, Superconductivity at 250 K in lanthanum hydride under high pressure, *Nature* **569**, 528 (2019).
  - [6] E. Snider, N. Dasenbrock-Gammon, R. McBride, M. Debessai, H. Vindana, K. Vencatasamy, K. V. Lawler, A. Salamat, and R. P. Dias, Room-temperature superconductivity in a carbonaceous sulfur hydride, *Nature* **586**, 373 (2020).
  - [7] L. Ma, K. Wang, Y. Xie, X. Yang, Y. Wang, M. Zhou, H. Liu, X. Yu, Y. Zhao, H. Wang, G. Liu, and Y. Ma, High-temperature superconducting phase in clathrate calcium hydride  $\text{CaH}_6$  up to 215 K at a pressure of 172 GPa, *Phys. Rev. Lett.* **128**, 167001 (2022).
  - [8] D. V. Semenov, A. G. Kvashin, A. G. Ivanova, V. Svitlyk, V. Y. Fomin, A. V. Sadakov, O. A. Sobolevskiy, V. M. Pudalov, I. A. Troyan, and A. R. Oganov, Superconductivity at 161 K in thorium hydride  $\text{ThH}_{10}$ : Synthesis and properties, *Materials Today* **33**, 36 (2020).
  - [9] P. Kong, V. S. Minkov, M. A. Kuzovnikov, A. P. Drodzov, S. P. Besedin, S. Mozaffari, L. Balicas, F. F. Balakirev, V. B. Prakapenka, S. Chariton, D. V. Semenov, E. Greenberg, and M. Eremets, Superconductivity up to 243 K in yttrium hydrides under high pressure, *Nature Communications* **12** (2021).
  - [10] I. A. Troyan, D. V. Semenov, A. G. Kvashin, A. V. Sadakov, O. A. Sobolevskiy, V. M. Pudalov, A. G. Ivanova, V. B. Prakapenka, E. Greenberg, A. G. Gavriliuk, V. V. Struzhkin, A. Bergara, I. Errea, R. Bianco, M. Calandra, F. Mauri, L. Monacelli, R. Akashi, and A. R. Oganov, Anomalous high-temperature superconductivity in  $\text{YH}_6$ , *Advanced Materials* **33**, 2006832 (2021).
  - [11] W. Chen, D. V. Semenov, X. Huang, H. Shu, X. Li, D. Duan, T. Cui, and A. R. Oganov, High-temperature superconducting phases in cerium superhydride with a  $T_c$  up to 115 K below a pressure of 1 Megabar, *Phys. Rev. Lett.* **127**, 117001 (2021).
  - [12] A. D. Grockowiak, M. Ahart, T. Helm, W. A. Coniglio, R. Kumar, K. Glazyrin, G. Garbarino, Y. Meng, M. Oliff, V. Williams, N. W. Ashcroft, R. J. Hemley, M. Somayazulu, and S. W. Tozer, Hot hydride superconductivity above 550 K, *Frontiers in Electronic Materials* **2** (2022).
  - [13] C. J. Pickard, I. Errea, and M. Eremets, Superconducting hydrides under pressure, *Annual Review of Condensed Matter Physics* **11**, 57 (2020).
  - [14] L. Boeri and G. B. Bachelet, Viewpoint: the road to room-temperature conventional superconductivity, *J. Phys.: Condens. Matter* **31**, 234002 (2019).
  - [15] J. A. Flores-Livas, L. Boeri, A. Sanna, G. Profeta, R. Arita, and M. Eremets, A perspective on conventional high-temperature superconductors at high pressure: Methods and materials, *Physics Reports* **856**, 1 (2020).
  - [16] S. D. Cataldo, C. Heil, W. von der Linden, and L. Boeri,  $\text{LaBH}_3$ : towards high- $T_c$  low-pressure superconductivity in ternary superhydrides, *Phys. Rev. B* **104**, L020511 (2021).
  - [17] R. Lucrezi, S. Di Cataldo, W. von der Linden, L. Boeri, and C. Heil, In-silico synthesis of lowest-pressure high- $T_c$  ternary superhydrides, *NPJ: computational materials* **8** (2022).
  - [18] S. D. Cataldo, W. von der Linden, and L. Boeri, Phase diagram and superconductivity of calcium borohydrides at extreme pressures, *Phys. Rev. B* **102**, 014516 (2020).
  - [19] Z. Zhang, T. Cui, M. J. Hutcheon, A. M. Shipley, H. Song, M. Du, V. Z. Kresin, D. Duan, C. J. Pickard, and Y. Yao, Design principles for high temperature superconductors with hydrogen-based alloy backbone at moderate pressure, *Physical Review Letters* **128** (2022).
  - [20] K. P. Hilleke and E. Zurek, Rational design of superconducting metal hydrides via chemical pressure tuning, arXiv preprint, arXiv:2205.11569 (2022).
  - [21] E. A. Ekimov, V. A. Sidorov, E. D. Bauer, N. N. Mel'nik, N. J. Curro, J. D. Thompson, and S. M. Stishov, Superconductivity in diamond, *Nature* **428**, 542 (2004).
  - [22] V. A. Sidorov and E. A. Ekimov, Superconductivity in diamond, *Diamond and Related Materials* **19**, 351 (2010).
  - [23] X. Cui, K. P. Hilleke, X. Wang, M. Lu, M. Zhang, E. Zurek, W. Li, D. Zhang, Y. Yan, and T. Bi,  $\text{RbB}_3\text{Si}_3$ : An alkali metal borosilicide that is metastable and superconducting at 1 atm, *Journal of Physical Chemistry C* **124** (2020).
  - [24] J. A. Flores-Livas, A. Sanna, M. Grauzinyte, A. Davydov, S. Goedecker, and M. A. L. Marques, Emergence of superconductivity in doped  $\text{H}_2\text{O}$  ice at high pressure, *Scientific Reports* **7**, 6825 (2017).
  - [25] H. Rosner, A. Kitaigorodsky, and W. E. Pickett, Prediction of high  $T_c$  superconductivity in hole-doped LiBC, *Phys. Rev. Lett.* **88**, 127001 (2002).
  - [26] S. Saha, S. D. Cataldo, M. Amsler, W. von der Linden, and L. Boeri, High-temperature conventional superconductivity in the boron-carbon system: Material trends, *Phys. Rev. B* **102**, 024519 (2020).
  - [27] S. D. Cataldo, S. Qulaghasi, G. B. Bachelet, and L. Boeri, High- $T_c$  superconductivity in doped boron-carbon clathrates, *Physical Review B* **105** (2022).
  - [28] J. Kortus, I. I. Mazin, K. D. Belashchenko, V. P. Antropov, and L. L. Boyer, Superconductivity of metallic boron in  $\text{MgB}_2$ , *Phys. Rev. Lett.* **86**, 4656 (2001).
  - [29] L. Boeri, J. Kortus, and O. K. Andersen, Three-dimensional  $\text{MgB}_2$ -type superconductivity in hole-doped diamond, *Phys. Rev. Lett.* **93**, 237002 (2004).
  - [30] T. A. Strobel, Abstract: S24.00003: Superconductivity in carbon-boron clathrates (2022), aPS Match Meeting 2022.
  - [31] S. Ichi Orimo, Y. Nakamori, J. R. Eliseo, A. Züttel, and C. M. Jensen, Complex hydrides for hydrogen storage, *Chem. Rev.* **107**, 4111 (2007).
  - [32] S.-W. Li, Y. Yan, S. Ichi Orimo, A. Züttel, and C. M. Jensen, Recent progress in metal borohydrides for hydrogen storage, *Energies* **4**, 185 (2011).
  - [33] Y. Filinchuk, E. Rönnebro, and D. Chandra, Crystal structures and phase transformations in  $\text{Ca}(\text{BH}_4)_2$ , *Acta Materialia* **57**, 732 (2009).
  - [34] A. Devos and M. Lannoo, Electron-phonon coupling for aromatic molecular crystals: Possible consequences for their superconductivity, *Phys. Rev. B* **58**, 8236 (1998).

- [35] R. Mitsuhashi, Y. Suzuki, Y. Yamanari, H. Mitamura, T. Kambe, N. Ikeda, H. Okamoto, A. Fujiwara, M. Yamaji, N. Kawasaki, Y. Maniwa, and Y. Kubozono, Superconductivity in alkali-metal-doped picene, *Nature* **464**, 76 (2010).
- [36] A. Subedi and L. Boeri, Vibrational spectrum and electron-phonon coupling of doped solid picene from first principles, *Phys. Rev. B* **84**, 020508 (2011).
- [37] M. Casula, M. Calandra, and F. Mauri, Local and nonlocal electron-phonon couplings in  $k_3$  picene and the effect of metallic screening, *Phys. Rev. B* **86**, 075445 (2012).
- [38] G. Savini, A. C. Ferrari, and F. Giustino, First-principles prediction of doped graphane as a high-temperature electron-phonon superconductor, *Phys. Rev. Lett.* **105**, 037002 (2010).
- [39] J. A. Flores-Livas, M. Grauzinyte, L. Boeri, G. Profeta, and A. Sanna, Superconductivity in doped polyethylene at high pressure, *The European Physical Journal B* **91**, 176 (2018).
- [40] J. E. Moussa and M. L. Cohen, Using molecular fragments to estimate electron-phonon coupling and possible superconductivity in covalent materials, *Phys. Rev. B* **78**, 064502 (2008).
- [41] S. Baroni, S. de Gironcoli, A. D. Corso, and P. Giannozzi, Phonons and related crystal properties from density-functional perturbation theory, *Rev. Mod. Phys.* **73**, 515 (2001).
- [42] Calculations were performed using DFPT as implemented in Quantum Espresso. Integration of electron-phonon properties was performed on  $3 \times 3 \times 3$  grid for phonons and  $16 \times 16 \times 16$  grid for electrons, using a Gaussian smearing of 200 meV. Further computational details are provided in the Supplementary Material [41, 44, 49–53].
- [43] C. Freysoldt, B. Grabowski, T. Hickel, and J. Neugebauer, First-principles calculations for point defects in solids, *Reviews of Modern Physics* **86**, 253 (2014).
- [44] `URL_will_be_inserted_by_publisher`, the supplementary material is available at..
- [45] For Ca and K we assumed a face-centered and a body-centered cubic structure, respectively.
- [46] M. D. Riktor, M. H. Sorby, K. Chlopek, M. Fichtner, F. Buchter, A. Züttel, and B. C. Hauback, *In situ* synchrotron diffraction studies of phase transitions and thermal decomposition of  $\text{Mg}(\text{BH}_4)_2$  and  $\text{Ca}(\text{BH}_4)_2$ , *Journal of Materials Chemistry* **17**, 4939 (2007).
- [47] J.-H. Kim, S.-A. Jin, J.-H. Shim, and Y. W. Cho, Thermal decomposition behavior of calcium borohydride  $\text{Ca}(\text{BH}_4)_2$ , *Journal of Alloys and Compounds* **461**, L20 (2008).
- [48] C. J. Sahle, C. Sternemann, C. Giacobbe, Y. Yan, C. Weis, M. Harder, Y. Forov, G. Spiekermann, M. Tolan, M. Krisch, and A. Remhof, Formation of  $\text{CaB}_6$  in the thermal decomposition of the hydrogen storage material  $\text{Ca}(\text{BH}_4)_2$ , *Phys. Chem. Chem. Phys.* **18**, 19866 (2016).
- [49] G. Kresse and J. Furthmüller, Efficient iterative schemes for *ab-initio* total-energy calculations using a plane-wave basis set, *Phys. Rev. B* **54**, 11169 (1996).
- [50] K. Momma and F. Izumi, VESTA: a three-dimensional visualization system for electronic and structural analysis, *J. Appl. Cryst.* **41**, 653 (2008).
- [51] P. Giannozzi, S. Baroni, N. Bonini, M. Calandra, R. Car, C. Cavazzoni, D. Ceresoli, G. L. Chiarotti, M. Cococcioni, and I. Dabo, QUANTUM ESPRESSO: a modular and open-source software project for quantum simulation of materials, *J. Phys.: Condens. Matter* **21**, 395502 (2009).
- [52] P. Giannozzi, O. Andreussi, T. Brumme, O. Bunau, M. B. Nardelli, M. Calandra, R. Car, C. Cavazzoni, D. Ceresoli, M. Cococcioni, N. Colonna, I. Carnimeo, A. D. Corso, S. de Gironcoli, P. Delugas, R. A. DiStasio, A. Ferretti, A. Floris, G. Fratesi, G. Fugallo, R. Gebauer, U. Gerstmann, F. Giustino, T. Gorni, J. Jia, M. Kawamura, H.-Y. Ko, A. Kokalj, E. Küçükbenli, M. Lazzeri, M. Marsili, N. Marzari, F. Mauri, N. L. Nguyen, H.-V. Nguyen, A. O. de-la Roza, L. Paulatto, S. Poncé, D. Rocca, R. Sabatini, B. Santra, M. Schlipf, A. P. Seitsonen, A. Smogunov, I. Timrov, T. Thonhauser, P. Umari, N. Vast, X. Wu, and S. Baroni, Advanced capabilities for materials modelling with quantum espresso, *J. Phys.: Condens. Matter* **29**, 465901 (2017).
- [53] D. R. Hamann, Optimized norm-conserving vanderbilt pseudopotentials, *Phys. Rev. B* **88**, 085117 (2017).